Journal of Porphyrins and Phthalocyanines
J. Porphyrins Phthalocyanines 2023; **27**: 569–575
DOI: 10.1142/S1088424623500396

Published at https://www.worldscinet.com/jpp/

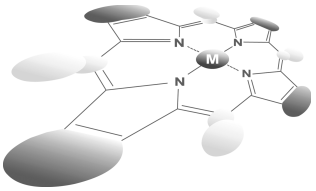

Photophysical characterization of a bisacridinium-diphenylporphyrin conjugate

Federica Ruani[a], Amy Edo-Osagie[b], Henri-Pierre Jacquot de Rouville[b], Valérie Heitz[◊,*,b], Barbara Ventura[◊,a], and Nicola Armaroli[*,a]

[a]*Istituto ISOF-CNR, Via P. Gobetti 101, 40129 Bologna, Italy*
[b]*Laboratoire de Synthèse des Assemblages Moléculaires Multifonctionnels, Institut de Chimie de Strasbourg, CNRS/UMR 7177, 4, rue Blaise Pascal, 67000 Strasbourg, France*

Received 21 November 2022
Accepted 20 January 2023

Dedicated to Prof. Tomás Torres on the occasion of his 70th birthday

ABSTRACT: A molecular conjugate made of a free-base diphenyl porphyrin chromophore (DPP) *trans*-linked to two N-acridinium units has been synthesized and photophysically characterized in acetonitrile. Interestingly, the emission of both fluorophores is quenched in the array at room temperature. Steady-state and time-resolved optical analysis proved that an ultrafast electron transfer from the porphyrin to the acridinium units occurs upon excitation of either the porphyrin or the acridinium moiety. On the other hand, at low temperature (77 K) the emission of the porphyrin is completely recovered, thanks to the inhibition of the electron transfer, and a photoinduced energy transfer from the acridinium to the porphyrin component is observed.

KEYWORDS: diphenyl-porphyrin, N-methylacridinium, photophysics, electron transfer, energy transfer.

INTRODUCTION

Porphyrins are naturally occurring and highly colored molecules whose extended π-conjugated system and metal chelating capacity make them widely abundant chromophores and ligands in biological systems [1–3]. One of the most interesting properties of this family of macrocycles is the possibility to tune their oxidation and reduction potentials by appending a variety of organic fragments or by changing the metal ion, which makes them widely used moieties in multicomponent systems undergoing photoinduced electron transfer [4–8]. This feature, along with the characteristic and rich photophysical behavior, make them suitable for use as molecular wires or switches, or in the fabrication of transistors, chemical sensors, and photodiodes [4, 9–12].

N-acridinium ions are intensively investigated as a new class of switches thanks to their responsiveness to various orthogonal stimulations – including pH or electrochemical/photochemical inputs – that trigger their reversible conversion into acridane [13–16]. Previous studies have demonstrated that the acridinium/acridane equilibrium significantly alters the photo- and electrochemical properties of supramolecular systems carrying those moieties [13, 17–20].

Previously, N-acridinium moieties have been associated with porphyrin chromophores in supramolecular systems, and those arrays could act as sensors or receptors [20–22]. Interestingly, in such systems a photoinduced electron transfer takes place from the porphyrin to the acridinium moiety, resulting in a quenching of both fluorophores. In this paper, a full photophysical investigation of a new molecular array

[◊]SPP full member in good standing.

*Correspondence to: Valérie Heitz, e-mail: v.heitz@unistra.fr, Tel: 33(0)368851357; Nicola Armaroli, e-mail: nicola.armaroli@isof.cnr.it, Tel: 0039 051 6399820.

(**1·(PF$_6$)$_2$**) composed of a free-base diphenyl-porphyrin moiety linearly connected to two N-acridinium units has been performed in acetonitrile (CH_3CN).

EXPERIMENTAL

Synthesis

All chemicals were of the best commercially available grade and used without further purification. All compounds were synthesized using schlenk technics and were fully characterized by 1D (^{1}H, ^{13}C{^{1}H}, ^{31}P{^{1}H} and ^{19}F{^{1}H}) and 2D (COSY, HSQC, and HMBC) NMR experiments and by mass spectrometry experiments. Nuclear magnetic resonance (NMR) spectra for ^{1}H were acquired on Bruker AVANCE 300 and 500 spectrometers. ^{13}C spectra were acquired on a Bruker AVANCE 500 spectrometer. ^{19}F spectra and 31P were acquired on a Bruker AVANCE 300 spectrometer. The ^{1}H and ^{13}C spectra were referenced to residual solvent peaks [23]. The sample was thermostated at 298 K unless otherwise stipulated. Mass spectra were obtained by using a Bruker MicroTOF spectrometer in electrospray mode (ESI).

Compound **1·(PF$_6$)$_2$**: To a solution of 9-(4-formylphenyl)-10-methylacridin-10-ium hexafluorophosphate [21] (554 mg, 1.25 mmol, 1 eq.) and dipyrromethane (183 mg, 1.25 mmol, 1 eq.) in degassed CH_2Cl_2 (250 mL) was added TFA (60.0 µL, 0.75 mmol, 0.6 eq.). The solution was left to stir in the dark for four hours, before neutralizing with Et_3N (2 mL). Following the removal of the solvent, the resultant solid was taken up in CH_3CN (100 mL) and DDQ (426 mg, 1.88 mmol, 1.5 eq.) was added to the solution. After stirring for one hour, purification was carried out via column chromatography (SiO_2, acetone/aq. KPF_6 soln., 100:0 to 95:5, R_f = 0.36) giving **1·(PF$_6$)$_2$** as a dark purple solid (203 mg, 29%). **^{1}H NMR** (500 MHz, CD_3CN, 298 K) δ (ppm) = 10.65 (s, 2H, H_{meso}), 9.72 (d, ^3J = 4.6 Hz, 4H, H_{py1}), 9.45 (d, ^3J = 4.6 Hz, 4H, H_{py2}), 8.75 (d, ^3J = 9.2 Hz, 4H, $H_{4/5}$), 8.68 (d, ^3J = 8.2 Hz, 4H, H_o), 8.66 (dd, ^3J = 8.7 Hz, ^4J = 1.3 Hz, 4H, $H_{1/8}$), 8.55 (ddd, ^3J = 9.2 & 6.6 Hz, ^4J = 1.3 Hz, 4H, $H_{3/6}$), 8.14 (ddd, ^3J = 8.7 & 6.6 Hz, ^4J = 0.8 Hz, 4H, $H_{2/7}$), 8.04 (d, ^3J = 8.2 Hz, 4H, H_m), 4.96 (s, 6H, CH_3), -3.09 (s, 2H, internal NH). **^{13}C{^{1}H} NMR** (125 MHz, CD_3CN, 298 K) δ (ppm) = 162.7 (C_9), 146.0 (CC_{py}), 144.1 (CC_o), 142.8 ($CC_{4/5}$), 139.9 ($C_{3/6}$), 135.8 (C_o), 134.0 (CC_m), 133.6 (C_{py1}), 132.2 (C_{py2}), 131.7 ($C_{1/8}$), 129.9 (C_m), 129.0 ($C_{2/7}$), 127.4 ($CC_{1/8}$), 119.5 ($C_{4/5}$), 106.8 (C_{meso}), 39.8 (NCH_3). **^{31}P{^{1}H}** NMR (202 MHz, CD_3CN, 298 K) δ (ppm) = -144.43 (hept, $^1J_{P\text{-}F}$ = 706.4 Hz). **^{19}F{^{1}H}** NMR (470 MHz, CD_3CN, 298 K) δ (ppm) = −72.97 (d, $^1J_{P\text{-}F$ = 706.4 Hz). **UV-Vis:** (CH_3CN, 298 K) λ_{max}(nm) = 348 (ε L mol^{-1}cm^{-1} 36 400), 362 (60 100), 404 (267 000), 501 (17 700), 538 (9490), 575 (6800), 629 (4220). **HRMS (ESI-TOF):** m/z cald. for $C_{60}H_{42}N_6^{2+}$ 423.1730, found 423.1752 (100%, $[M\text{-}2PF_6]^{2+}$); m/z cald. for $C_{61}H_{42}N_7^{2+}$ 872.3502, found 872.3521 (80%, $[M\text{-}2PF_6\text{+}CN]^+$).

Absorption and emission spectroscopy, photophysics

Spectroscopic grade Uvasol® acetonitrile (CH_3CN) and butyronitrile ($CH_3CH_2CH_2CN$) were purchased from Merck and used without further purification. All standards were acquired from commercial suppliers and used without further purification: *meso*-tetraphenylporphyrin from Porphychem and Coumarin 153 from Sigma Aldrich. 5,15 diphenylporphyrin (**DPP**) model was purchased from Porphychem.

Absorption spectra were recorded with Perkin–Elmer Lambda 650 UV-vis or Lambda 950 UV-vis-NIR spectrophotometers in 1 cm quartz cuvettes. Emission spectra were collected with an Edinburgh FLS920 spectrofluorimeter, equipped with a Peltier-cooled Hamamatsu R928 PMT (280–850 nm).

Fluorescence quantum yields (Φ_{fl}) were evaluated from the comparative method developed by Demas and Crosby [24], with spectra corrected for the wavelength-dependent photomultiplier response. Air-equilibrated references used were *meso*-tetraphenylporphyrin (**TPP**) in toluene (Φ_{fl} = 0.11) [25] for the porphyrin components and Coumarin 153 in ethanol (Φ_{fl} = 0.544) [26] for the acridinium units. Measurements at 77 K were performed using Pyrex tubes dipped in liquid nitrogen in a quartz Dewar. Excitation spectra were corrected for the wavelength-dependent lamp intensity.

Emission lifetimes in the nanosecond range were determined by using an IBH time-correlated single-photon counting apparatus with nanoLED excitation sources at 465 nm and 368 nm.

Pump-probe transient absorption measurements were performed with an Ultrafast Systems HELIOS (HE-VIS-NIR) femtosecond transient absorption spectrometer by using, as an excitation source, a Newport Spectra Physics Solstice-F-1K-230 V laser system, combined with a TOPAS Prime (TPR-TOPAS-F) optical parametric amplifier (pulse width: 100 fs, 1 kHz repetition rate) tuned at 360 nm and 500 nm. A CaF_2 crystal for continuum generation in the UV-vis range (300–750 nm) has been employed. The overall time resolution of the system is 300 fs. Air-equilibrated solutions in 0.2 cm optical path cells were analyzed under continuous stirring. The pump energy on the sample was 4 µJ/pulse. Surface Xplorer V4 software from Ultrafast Systems was used for data acquisition and analysis. The 3D data surfaces were corrected for the chirp of the probe pulse before analysis.

Estimated errors are 10% on transient absorbance lifetimes, 10% for luminescence lifetimes, 10% for molar absorption coefficients, and 10% on quantum yields.

Free energy calculations ΔG_{CS} for electron transfer

The free energy for the charge-separation (ΔG_{CS}) occurring in **1·(PF$_6$)$_2$** from the singlet excites state of either the porphyrin or the acridinium has been calculated in CH_3CN through the semi-empirical Rehm-Weller equation (1) [27]:

$$\Delta G_{CS} = e[E^{ox} - E^{red}] - E_{00}(DPP/Acr^{+}) - \frac{e^2}{4\pi\varepsilon_0\varepsilon_s d}, \quad (1)$$

where E_{ox} and E_{red} are the oxidation potentials of the porphyrin unit (+1.15 V *vs* SCE) [28] and the reduction potential of the acridinium unit (-0.55 V *vs* SCE) [16], respectively, in CH_3CN; E_{00} *(DPP/Acr⁺)* is the energy of the singlet excited state of either the porphyrin (2.0 eV, Table 1) or the acridinium (2.5 eV, Table 1); *e* is the elementary charge (1.602×10^{-19} C); ε_0 is the vacuum permittivity (8.854×10^{-12} Fm^{-1}); ε_s is the permittivity of the solvent ($\varepsilon_s = 35.94$) and *d* is the donor-acceptor (D-A) separation.

The value for *d* (10.7 Å) has been obtained by approximating the D-A separation as a distance between the two centroids of the acridinium and the porphyrin components. The structures for these calculations have been obtained with the semi-empirical PM6 energy minimization.

The free energy for charge-recombination (ΔG_{CR}) has been obtained as the difference between E_{00} *(DPP)* and the energy of the charge-separated state (E_{CS}), the latter taken equal to the ΔG_{CS} with the opposite sign:

$$\Delta G_{CR} = E_{CS} - E_{00}(DPP). \quad (2)$$

RESULTS AND DISCUSSION

Photophysical investigation

The photophysical characterization of the multicomponent array **1·(PF$_6$)$_2$** and its moieties, i.e. 5,15-(diphenyl) porphyrin (**DPP**) and N-phenyl-acridinium (**Acr·PF$_6$**) (Chart 1) has been performed in acetonitrile (CH_3CN).

The absorption spectrum of the array has been compared with those of **Acr·PF$_6$** and **DPP** models. **Acr·PF$_6$** has a strong absorption in the UV with two characteristic peaks at 260 and 361 nm. **DPP** shows the typical absorption features of free-base porphyrins, with the Soret band at 400 nm and four Q bands at 500, 536, 575, and 627 nm. From the comparison of Fig. 1, a good match between the absorption of the array and the sum of the spectra of the three individual moieties (two **Acr⁺** units and one **DPP**) can be observed. In particular, the overlap is very good in the Q-bands region (470–650 nm) and on the acridinium peaks, while the Soret band of the array is less intense and broadened with respect to the porphyrin component. These features suggest weak ground-state electronic interactions between the components in the array.

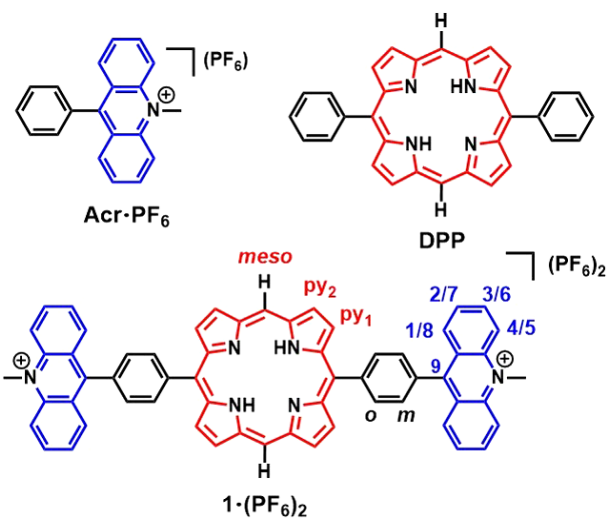

Chart 1. Chemical structures of the array **1·(PF$_6$)$_2$**, and models N-phenyl-acridinium (**Acr·PF$_6$**) and 5,15-(diphenyl)porphyrin (**DPP**).

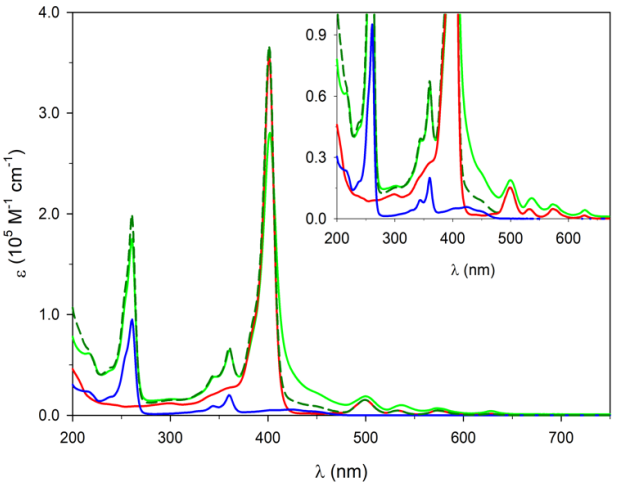

Fig. 1. Absorption spectra in CH_3CN of **1·(PF$_6$)$_2$** (light green), **Acr·PF$_6$** (blue), and **DPP** (red), along with a simulated spectrum (dark green dashed) given by the sum of the spectra of the three individual moieties (two **Acr⁺** and one **DPP**). Inset: amplification of the spectra in the 200–650 nm range.

Both models, **Acr·PF$_6$** and **DPP**, are fluorescent at room temperature (Φ_{em} and τ are reported in Table 1), but the conjugate **1·(PF$_6$)$_2$** was found to be weakly emissive at any excitation wavelength. Selective excitation of the **DPP** unit is possible for $\lambda > 470$ nm (Fig. 1), while it is not possible to selectively excite the acridinium moiety, although predominant excitation can be obtained at 260 or 361 nm. From selective excitation of the porphyrin at 500 nm, an almost complete quenching of its emission (> 99%) in the array can be observed (Fig. 2). On the other hand, also predominant excitation of the acridinium moiety at 361 nm (60% selectivity) results in its complete emission quenching in the array (Fig. S1, ESI). The experiment has been performed by comparing the emission spectra of solutions of the conjugate and models, the latter having the same number of photons absorbed by the corresponding moieties in the array. It can be noticed that also the porphyrin fluorescence is quenched with respect to that of the **DPP** model (Fig. S1, ESI). Based on previously studied systems, the observed quenching can be ascribed to a fast photoinduced electron transfer from the porphyrin to the acridinium component, affording the charge-separated species **Acr⁺-DPP$^{•+}$-Acr$^{•}$** [21]. To test

Table 1. Emission data of models and **1** in the indicated solvents and at the indicated temperatures.

		RT, CH_3CN			77 K, $CH_3CH_2CH_2CN$		
		λ_{max}^{em} (nm)	Φ_{em} [a]	τ [b] (ns)	λ_{max}^{em} (nm)	τ [b] (ns)	E [c] (eV)
DPP	^{1}DPP	632; 697	0.053	9.2	627; 694	15.0	2.0
Acr·PF$_6$	^{1}Acr$^+$	510	0.050	1.5	468; 500	3.4 (7%); 17.7 (93%)	2.5
1·(PF$_6$)$_2$	Acr$^+$-^{1}DPP [d,e]	634; 698	$<10^{-4}$	-	626; 693	15.9	2.0
	^{1}Acr$^+$-DPP [e]	-	$<10^{-4}$	-	-	-	-

[a]Fluorescence quantum yields, measured with the comparative method [24]. References used (air-equilibrated solutions): TPP (*meso*-tetraphenylporphyrin) in toluene for the porphyrin units; Coumarin 153 in ethanol for the acridinium units. [b]Fluorescence lifetimes in the nanosecond range, excitation wavelengths are 465 nm (porphyrin units), and 368 nm (acridinium moieties). [c]Energy of the excited state determined as the energy of the 0–0 emission band measured at 77 K. [d]Upon selective excitation of the diphenylporphyrin at 500 nm. [e] The yield is below the minimum value measurable with steady-state experiments, i.e., 1.0×10^{-4}.

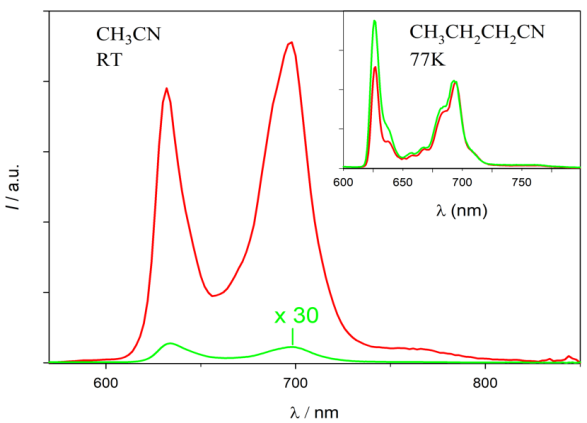

Fig. 2. Corrected luminescence spectra of isoabsorbing solutions of **DPP** (red) and **1·(PF$_6$)$_2$** (light green) in CH_3CN; λ_{exc} = 500 nm. Inset: corrected fluorescence spectra at 77 K in butyronitrile ($CH_3CH_2CH_2CN$) of isoabsorbing solutions of **DPP** (red) and conjugate (light green), upon selective excitation of the porphyrin moiety (λ_{exc} = 500 nm).

if an energy transfer process from the acridinium to the free-base porphyrin occurs, the excitation spectrum of the array has been collected at 704 nm (Fig. S4, ESI), where only emission from the porphyrin can be monitored. Comparison with the absorption spectrum of the array shows that the absorption peaks of the porphyrin moiety are well recovered in the excitation spectrum, while the peaks corresponding to the absorption of the acridinium units are not present. This indicates that energy transfer from the acridinium to the porphyrin is not taking place at room temperature.

Emission measurements were performed also at 77 K by dipping butyronitrile solutions of the compounds into liquid nitrogen. Upon selective excitation of the porphyrin units in the array (λ_{exc} = 500 nm) at 77 K, it was possible to observe a complete recovery of porphyrin emission (Fig. 2, inset), suggesting that the electron transfer process is disfavored because of the hampered solvent reorganization around the newly charged species that would be produced. Interestingly, the low-temperature excitation spectrum, collected at the porphyrin emission (λ_{em} = 626 nm), shows the presence of the absorption peaks of the acridinium units together with those of the porphyrin (Fig. S5, ESI), suggesting that energy transfer from the acridinium to the porphyrin takes place at 77 K when the fast electron transfer is inhibited. As a further confirmation, excitation of the acridinium moiety (λ_{exc} = 360 nm) at 77 K leads to observing a complete quenching of its emission in the conjugate, whereas the fluorescence of the acridinium model **Acr·PF$_6$** is very intense, also displaying a vibrational resolution (Fig. S2, ESI). On the other hand, the porphyrin-based emission in the array (Fig. S2, ESI) turns out to be intense and comparable to that of the **DPP** model, indicating sensitization of the singlet excited state of the porphyrin from the acridinium singlet.

Transient absorption spectroscopy

To ascertain the occurrence of a photoinduced electron transfer process within the units of the array, transient absorption (TA) measurements were performed on the array and the models for comparison purposes.

Upon excitation at 500 nm, the transient spectrum of the **DPP** model shows a positive absorption in the 450–800 nm region that sums with ground-state bleaching of the Q-bands at 500, 526, 575, and 627 nm and stimulated emission at ca. 630 and 700 nm (Fig. 3a), as usually detected for porphyrin species. Conversely, the TA signal observed in the conjugate (Fig. 3b) shows a more intense absorption between 520 and 800 nm, a region in which both the porphyrin cation and the reduced acridinium species absorb [16, 19, 21, 29–31], and a more defined band peaking at 470 nm, which can be attributed to the reduced acridinium [16, 19, 21, 31, 32]. The main unambiguous difference resides in the kinetics, since in the model the spectrum decays with a lifetime of *ca.* 10 nanoseconds (outside the maximum time scale of the instrument), in line with the lifetime of the singlet excited state of the porphyrin (Table 1), reaching a stable signal on a longer time scale that can be attributed to the triplet,

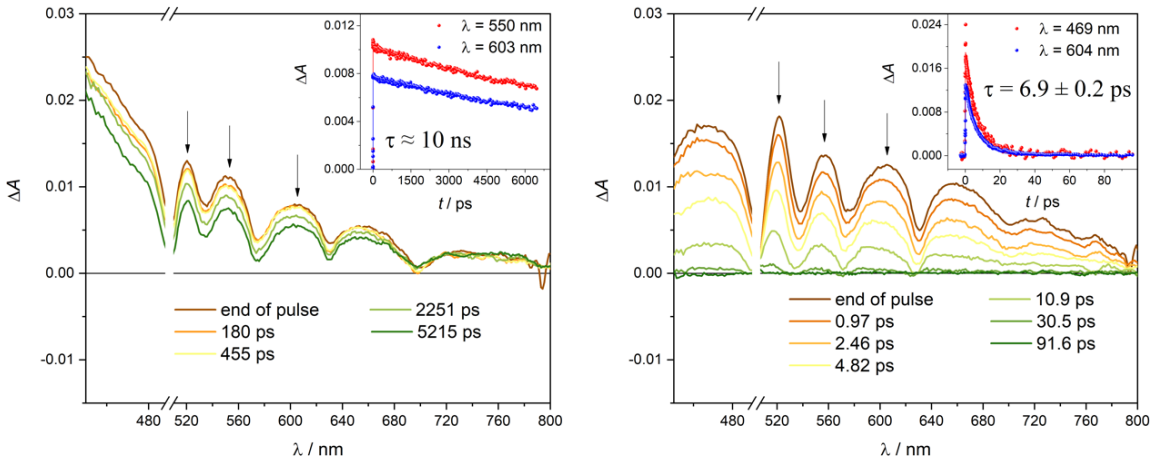

(a) (b)

Fig. 3. Transient absorption spectra of (a) **DPP** and (b) **1·(PF$_6$)$_2$** in CH_3CN at different delays. Excitation at 500 nm (A_{500} = 0.1, 0.2 cm optical path, 4 μJ/pulse). Insets: ΔA time evolutions (dots) and fittings (lines) at the indicated wavelengths.

while in the array the spectrum decays to zero in a much shorter time (τ = 6.9 ps). It can be thus concluded that the end-of-pulse spectrum detected in the conjugate is that of the charge-separated state, indicating that the process is ultrafast (occurring within the signal formation: 300 fs) and that charge-recombination occurs within about 7 ps.

Measurements upon acridinium prevalent excitation at 360 nm have also been made for the conjugate and models **Acr$^+$** and **DPP** (Fig. 4 and Fig. S3, ESI). The signal of model **Acr·PF$_6$** is very weak in this solvent (Fig. 4a) and shows positive absorption between 450 and 500 nm and stimulated emission in the 500–650 nm range. The observed decay is in line with the excited state lifetime found from luminescence measurements (Table 1). **DPP** shows features similar to those detected upon excitation at 500 nm (Fig. S3a, ESI), with kinetics well fitted by a two-exponential decay with lifetimes of about 4 ps and tens of ns. The first short lifetime might be related to a fast internal conversion process between S_2 and S_1, while the longer one is related to S_1 deactivation. The peaks observed for the conjugate (Fig. 4b) are similar to those of the porphyrin model, but with a more intense absorption between 640 and 800 nm. Again, the first band at ca. 480 nm is indicative of the presence of radical **Acr$^•$**, which displays bands between 480 and 520 nm [30]. On the other hand, the decay of the signal in the array is well-fitted by a lifetime of 6.4 ps.

Overall, it can be concluded that the features of the charge-separated state are present at the end-of-pulse both with the excitation of the porphyrin or of the acridinium component, indicating that charge separation occurs on ultrafast scales. Once the CS is formed, charge recombination takes place in ca. 6.5 ps. The free energy (ΔG_{CS}) for charge separation from the porphyrin singlet excited state is -0.3 eV (obtained by applying equation 1, Experimental Section), while from the acridinium singlet excited state is -0.8 eV (Scheme 1). It can be noticed that a similar ultrafast electron transfer process was observed

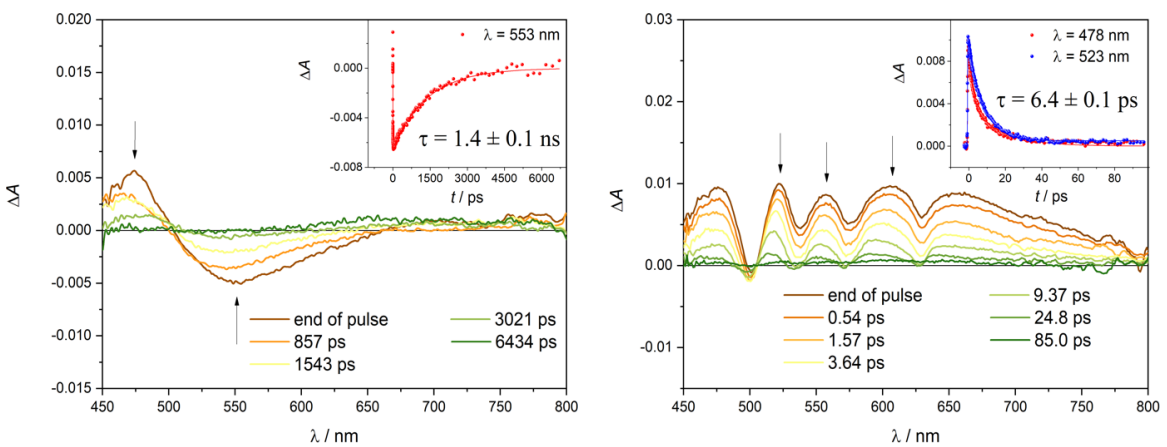

(a) (b)

Fig. 4. Transient absorption spectra of (a) N-phenyl-acridinium **Acr·PF$_6$** and (b) **1·(PF$_6$)$_2$** in CH_3CN at different delays. Excitation at 360 nm (A_{360} = 0.1, 0.2 cm optical path, 4 μJ/pulse). Insets: ΔA time evolutions (dots) and fittings (lines) at the indicated wavelengths.

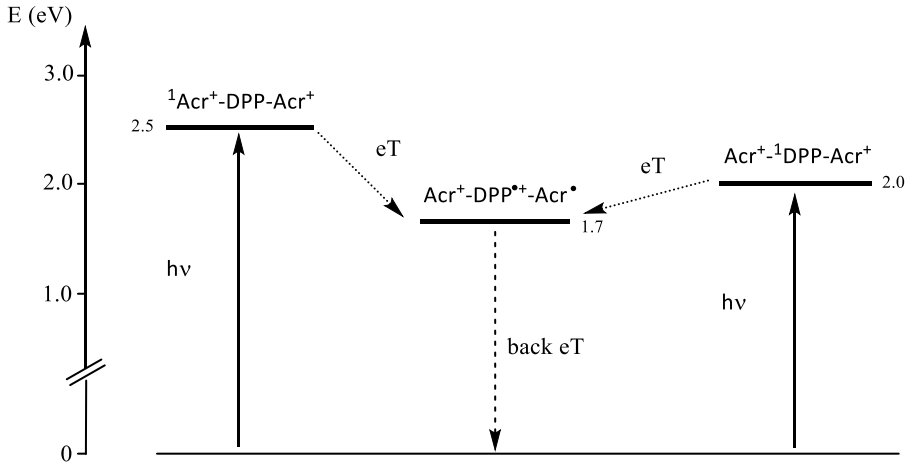

Scheme 1. Energy level diagram and photoinduced processes occurring in **1·(PF$_6$)$_2$** in CH_3CN solution at 298 K. The singlet energy levels are taken from the data of the present paper. The energy of the charge-separated state (1.7 eV) has been calculated according to equation 2 (see the Experimental Section).

in a related system incorporating a Zn(II) porphyrin instead of a free-base porphyrin [21]. The formation of the charge-separated state was detected on the same ultrafast scale (≤ 300 fs) for the Zn(II) porphyrin-containing conjugate, while the kinetics of the charge recombination reaction was faster, in the order of 1 ps, in accordance with a charge-separated state of lower energy, i.e. 1.39 eV. Notably, in supramolecular systems containing dimeric porphyrinic tweezer-like receptors complexing an acridinium guest [19, 22] an electron transfer process from the free-base porphyrins to the acridinium unit was observed but on longer timescales (few ns). The occurrence of ultrafast events in the present array can be ascribed to through a bond reaction between covalently linked units, differently from the reported supramolecular systems where a through space electron transfer is envisaged.

CONCLUSIONS

A multicomponent array made of a free-base diphenyl-porphyrin (**DPP**) chromophore covalently linked to two acridinium (**Acr$^+$**) moieties, upon excitation of either the porphyrin or the acridinium component, undergoes an ultrafast electron transfer process from the porphyrin to an acridinium unit, forming the charge-separated species **Acr$^+$-DPP$^{\bullet+}$-Acr$^\bullet$**. This process results in a quenching of both luminophores at room temperature and the charge-separated intermediate and related kinetics can be observed with femtosecond transient absorption spectroscopy. By decreasing the temperature to 77 K, charge separation is suppressed and the free-base porphyrin emission is recovered, upon its selective excitation. On the other hand, low-temperature excitation of the acridinium luminophore leads to its quenching, with concomitant sensitization of the porphyrin fluorescence. These results suggest that the present bis-acridinium free-base porphyrin conjugate and related arrays containing metallated porphyrins are promising donor-acceptor systems for the development of molecular wires or the design of temperature-sensitive probes.

Acknowledgments

The work is supported by the H2020-MSCA-ITN-2017-765297 project "NOAH" and by the H2020-LC-SC3-2020-RES-RIA-101006839 project "CONDOR". Special thanks go to the Italian CNR (PHEEL project).

Supporting information

Figures S1–S15 are given in the supplementary material. This material is available free of charge *via* the Internet at https://www.worldscientific.com/doi/suppl/10.1142/S1088424623500396

REFERENCES

1. Smith KM. 1.23 - Porphyrins, *Comprehensive Coordination Chemistry II* (McCleverty JA and Meyer TJ, eds.) 2003; 493–506.
2. Wang Z, Yang C, Yang Z, Brown CE, Hollebone BP and Stout SA. 4 - Petroleum biomarker fingerprinting for oil spill characterization and source identification, *Standard Handbook Oil Spill Environmental Forensics (Second Edition)* Stout SA,Wang Z, 2016; 131–254.
3. Mortimer RJ and Rowley NM. Metal complexes as dyes for optical data storage and electrochromic materials, *Comprehensive Coordination Chemistry II.* 2004; 581–619.
4. Jurow M, Schuckman AE, Batteas JD and Drain CM. *Coord. Chem. Rev.* 2010; **254**: 2297–2310.
5. Drain CM, Varotto A and Radivojevic I. *Chem. Rev.* 2009; **109**: 1630–1658.

6. Wasielewski MR. *J. Org. Chem.* 2006; **71**: 5051–5066.
7. Hayes RT, Wasielewski MR and Gosztola D. *J. Am. Chem. Soc.* 2000; **122**: 5563–5567.
8. Wang Y, Wang X, Ghosh SK and Lu HP. *J. Am. Chem. Soc.* 2009; **131**: 1479–1487.
9. Burrell AK and Wasielewski MR. *J. Porphyr. Phthalocya.* 2000; **4**: 401–406.
10. Paolesse R, Nardis S, Monti D, Stefanelli M and Di Natale C. *Chem. Rev.* 2017; **117**: 2517–2583.
11. Lindsey JS and Bocian DF. *Acc. Chem. Res.* 2011; **44**: 638–650.
12. Beletskaya I, Tyurin VS, Tsivadze AY, Guilard R and Stern C. *Chemical Reviews* 2009; **109**: 1659–1713.
13. Jacquot de Rouville HP, Hu J and Heitz V. *Chempluschem* 2021; **86**: 110–129.
14. Raskosova A, Stosser R and Abraham W. *Chem. Commun.* 2013; **49**: 3964–3966.
15. Xie Y, Ilic S, Skaro S, Maslak V and Glusac KD. *J. Phys. Chem. A* 2017; **121**: 448–457.
16. Fukuzumi S, Ohkubo K, Suenobu T, Kato K, Fujitsuka M and Ito O. *J. Am. Chem. Soc.* 2001; **123**: 8459–8467.
17. Abraham W, Buck K, Orda-Zgadzaj M, Schmidt-Schaffer S and Grummt UW. *Chem. Commun.* 2007; 3094–3096.
18. Vetter A and Abraham W. *Org. Biomol. Chem.* 2010; **8**: 4666–4681.
19. Tanaka M, Ohkubo K, Gros CP, Guilard R and Fukuzumi S. *J. Am. Chem. Soc.* 2006; **128**: 14625–14633.
20. Kotani H, Ohkubo K, Crossley MJ and Fukuzumi S. *J. Am. Chem. Soc.* 2011; **133**: 11092–11095.
21. Edo-Osagie A, Sanchez-Resa D, Serillon D, Bandini E, Gourlaouen C, de Rouville HPJ, Ventura B and Heitz V. *Cr. Chim.* 2021; **24**: 47–55.
22. Chaudhary A and Rath SP. *Chem. Eur. J.* 2012; **18**: 7404–7417.
23. Fulmer GR, Miller AJM, Sherden NH, Gottlieb HE, Nudelman A, Stoltz BM, Bercaw JE and Goldberg KI. *Organometallics* 2010; **29**: 2176–2179.
24. Demas JN and Crosby GA. *J. Phys. Chem-Us* 1971; **75**: 991–1242.
25. Seybold PG and Gouterman M. *J. Mol. Spectrosc.* 1969; **31**: 1–13.
26. Rurack K and Spieles M. *Anal. Chem.* 2011; **83**: 1232–1242.
27. Williams RM, Koeberg M, Lawson JM, An YZ, Rubin Y, PaddonRow MN and Verhoeven JW. *J. Org. Chem.* 1996; **61**: 5055–5062.
28. Marcille H, Malval JP, Presset M, Bogliotti N, Blacha-Grzechnik A, Brezova V, Yagci Y and Versace DL. *Polym. Chem-Uk* 2020; **11**: 4237–4249.
29. Aleman EA, Manriquez Rocha J, Wongwitwichote W, Godinez Mora-Tovar LA and Modarelli DA. *J. Phys. Chem. A* 2011; **115**: 6456–6471.
30. Benniston AC, Harriman A, Li PY, Rostron JP, van Ramesdonk HJ, Groeneveld MM, Zhang H and Verhoeven JW. *J. Am. Chem. Soc.* 2005; **127**: 16054–16064.
31. Ohkubo K, Suga K, Morikawa K and Fukuzumi S. *J. Am. Chem. Soc.* 2003; **125**: 12850–12859.
32. Tanaka M, Ohkubo K, Gros CP, Guilard R and Fukuzumi S. *ECS Trans.* 2007; **2**: 167–176.